Supporting Information to:

Indium-modified Copper nanocubes for syngas production from aqueous CO_2 electroreduction

Alessandro Niorettini[1], Raffaello Mazzaro[2,3,*], Fabiola Liscio[3], Alessandro Kovtun[4], Luca Pasquini[2], Stefano Caramori[1], Serena Berardi[1,*]

[1] Department of Chemical, Pharmaceutical and Agricultural Sciences, University of Ferrara, Via Luigi Borsari 46, 44121 Ferrara, Italy.

[2] Department of Physics and Astronomy, University of Bologna, Via Berti Pichat 6/2 Bologna, Italy.

[3] CNR-IMM, Via Piero Gobetti 101, Bologna, Italy.

[4] CNR-ISOF, Via Piero Gobetti 101, Bologna, Italy.

[*] Corresponding author: serena.berardi@unife.it

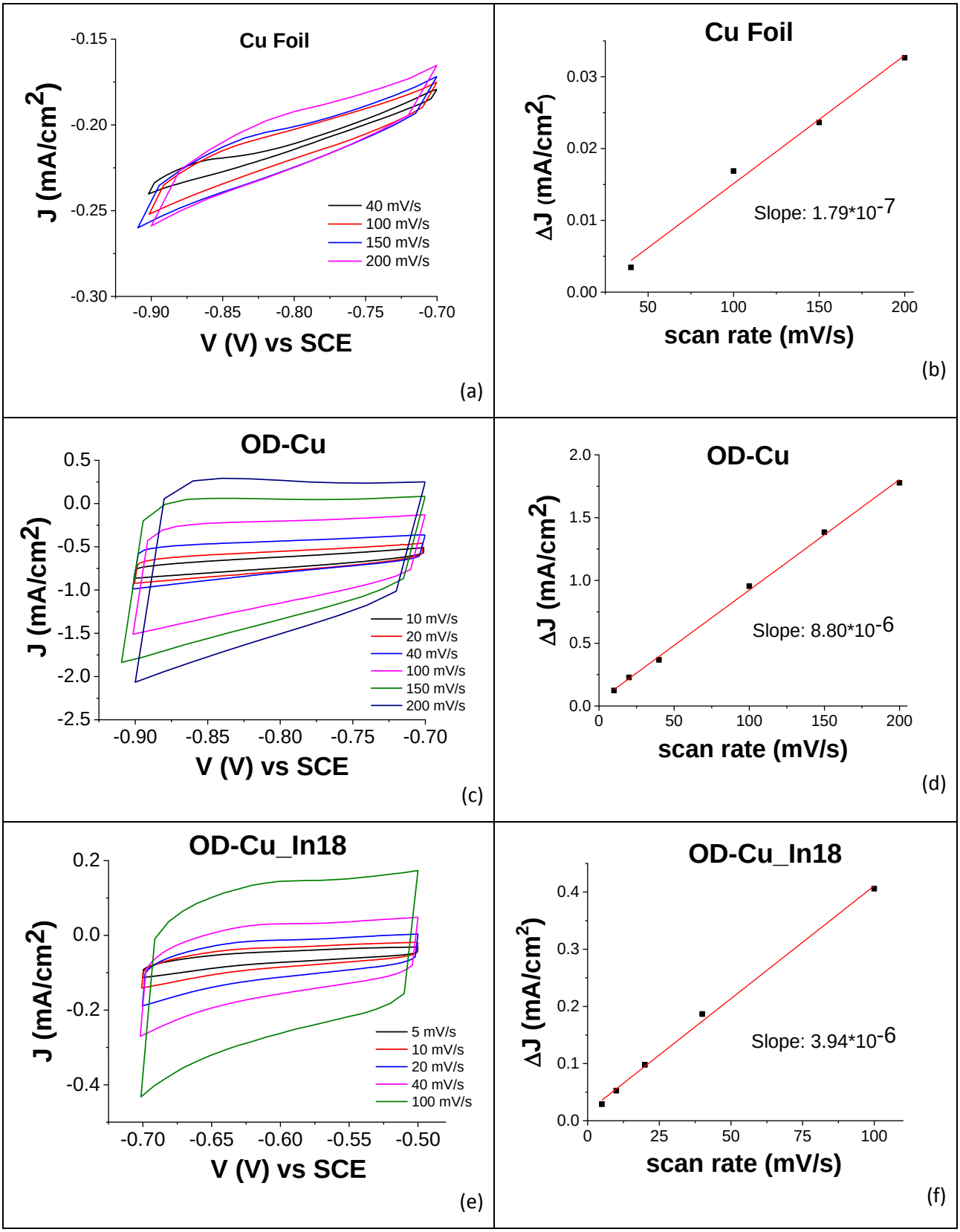
Cu Foil
J (mA/cm2)
V (V) vs SCE
40 mV/s
100 mV/s
150 mV/s
200 mV/s
(a)
Cu Foil
ΔJ (mA/cm2)
scan rate (mV/s)
Slope: 1.79*10-7
(b)
OD-Cu
J (mA/cm2)
V (V) vs SCE
10 mV/s
20 mV/s
40 mV/s
100 mV/s
150 mV/s
200 mV/s
(c)
OD-Cu
ΔJ (mA/cm2)
scan rate (mV/s)
Slope: 8.80*10-6
(d)
OD-Cu_In18
J (mA/cm2)
V (V) vs SCE
5 mV/s
10 mV/s
20 mV/s
40 mV/s
100 mV/s
(e)
OD-Cu_In18
ΔJ (mA/cm2)
scan rate (mV/s)
Slope: 3.94*10-6
(f)

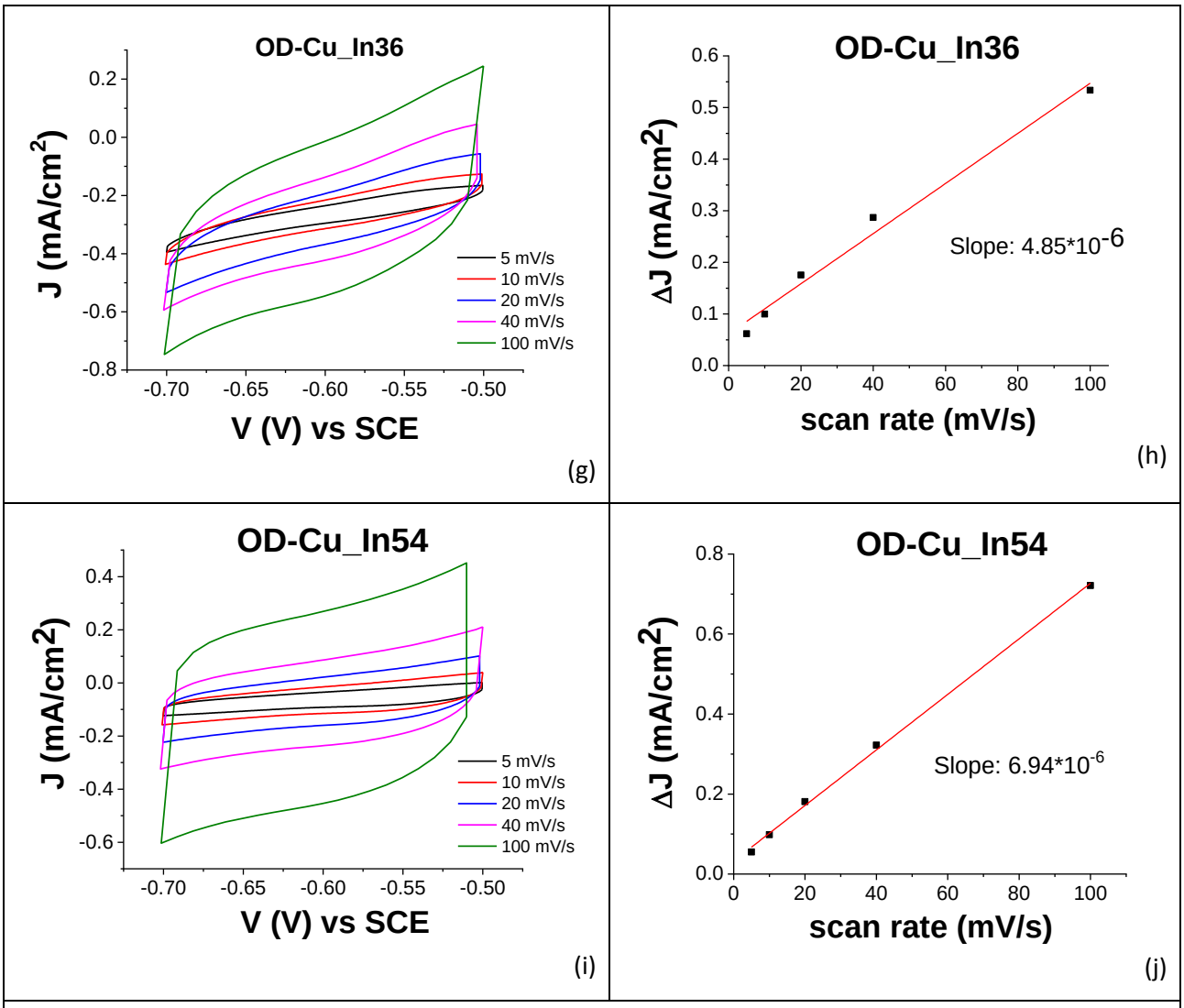

Figure S1. CV scans for the electrochemical surface area (ECSA) determination for Cu foil **(a)**, OD-Cu **(c)**, OD-Cu_In18 **(e)**, OD-Cu_In36 **(g)**, and OD-Cu_In54 **(i)** registered in 0.1 M aqueous $KHCO_3$. The corresponding linear fits for the determination of electrode capacitance are reported respectively in **(b)**, **(d)**, **(f)**, **(h)** and **(j)**. The corresponding roughness factor (RF) values are reported in Table S1.

Table S1. Average values of the electrodes capacitance (*i.e.* the slope of the plots in Figure S1b, d, f, h and j) and the corresponding roughness factors.

Electrode	Capacitance (µF)	Roughness Factor
Cu foil	0.179	1
OD-Cu	8.8	50
OD-Cu_In18	3.94	22
OD-Cu_In36	4.85	27
OD-Cu_In54	6.94	39

X-Ray Photoelectron Spectroscopy:

Atomic composition and binding energy of the main transition of OD-Cu, OD-Cu_In36 and OD-Cu_In36_post are reported in Table S2.

Table S2. XPS atomic composition (at. %) of OD-Cu, OD-Cu_In36 and OD-Cu_In36_post.

Transition	C 1s	O 1s	Cu 2p	Cu 2p	Cu 2p	In 3d	K 2p
Chemical state	C-C	various	Cu(0)	Cu(I)	Cu(II)	In(III)*	K^+
Binding energy	285.1eV	532 eV	932.5eV	932.5eV	934.4 eV	445.2eV	293.1eV
OD-Cu	44.4 ±1.0	38.5 ±1.0	-	7.1 ±0.3	0.7 ±0.2	-	9.3 ±0.5
OD-Cu_ In36	43.8 ±1.0	51.2 ±1.0	-	0.9 ±0.2	2.3 ±0.3	1.8 ±0.1	-
OD-Cu_ In36_post	53.0 ±1.0	32.0 ±0.5	2.8 ±0.4	**	0.6 ±0.2	0.8 ±0.1	10.8 ±0.5

* In 3d 5/2 presents a relative shift between OD-Cu_In36 (445.2 eV) and OD-Cu_In36_post (444.9 eV), that corresponds to $In(OH)_3$ and In_2O_3 respectively.

** Metallic Cu(0) and Cu(I) present the same binding energy, only from Cu LMM signal is possible to qualitatively confirm the presence of both.

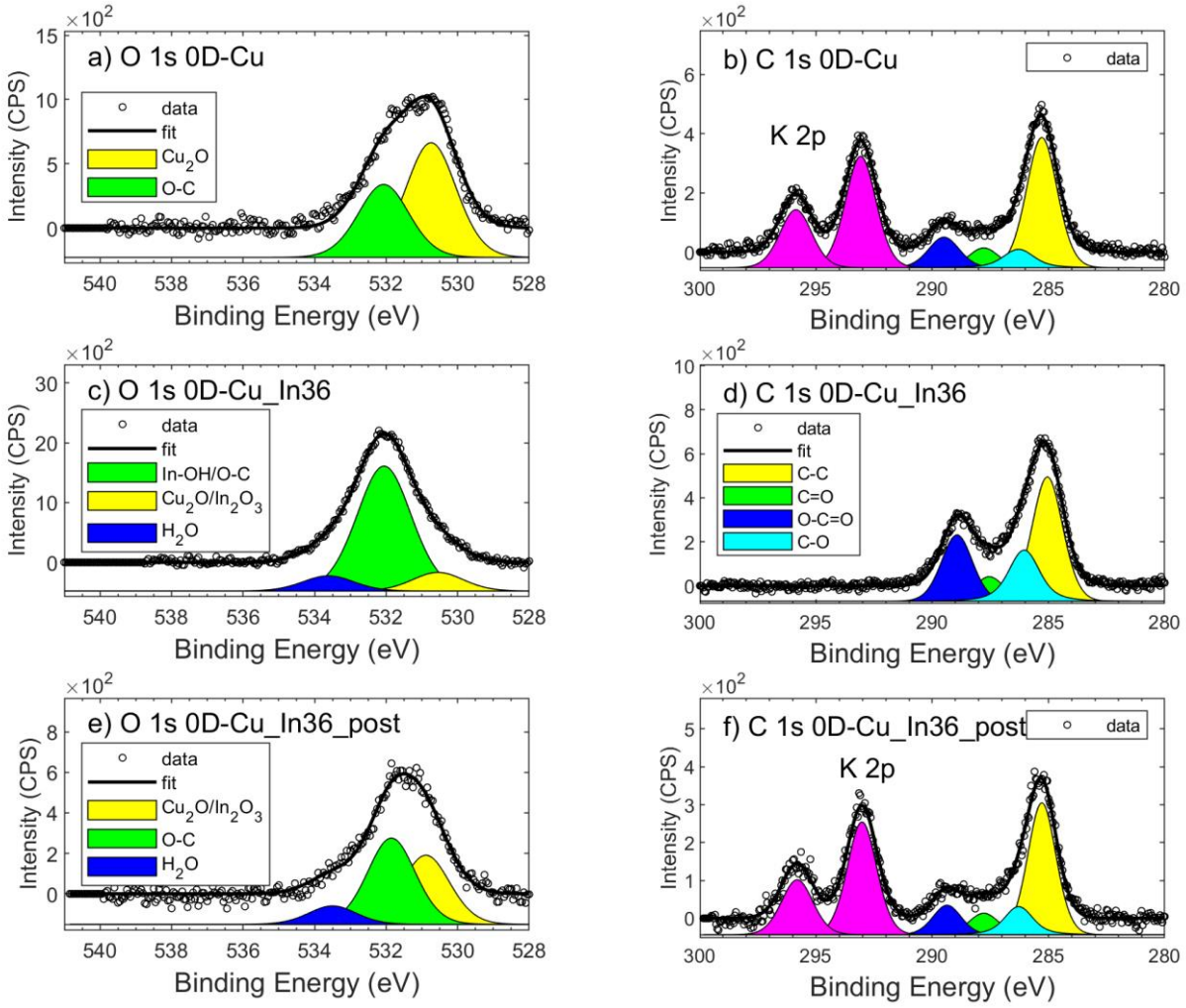

Figure S2. XPS signals of O 1s **(a-c-e)** and C 1s **(b-d-f)**. K 2p signal was found only in OD-Cu and OD-Cu_In36_post (doublet in magenta). In **(c)** the In-OH/O-C peak considers both the contribution of oxygen in carbonate and the hydroxides forms of In (as well as of Cu).

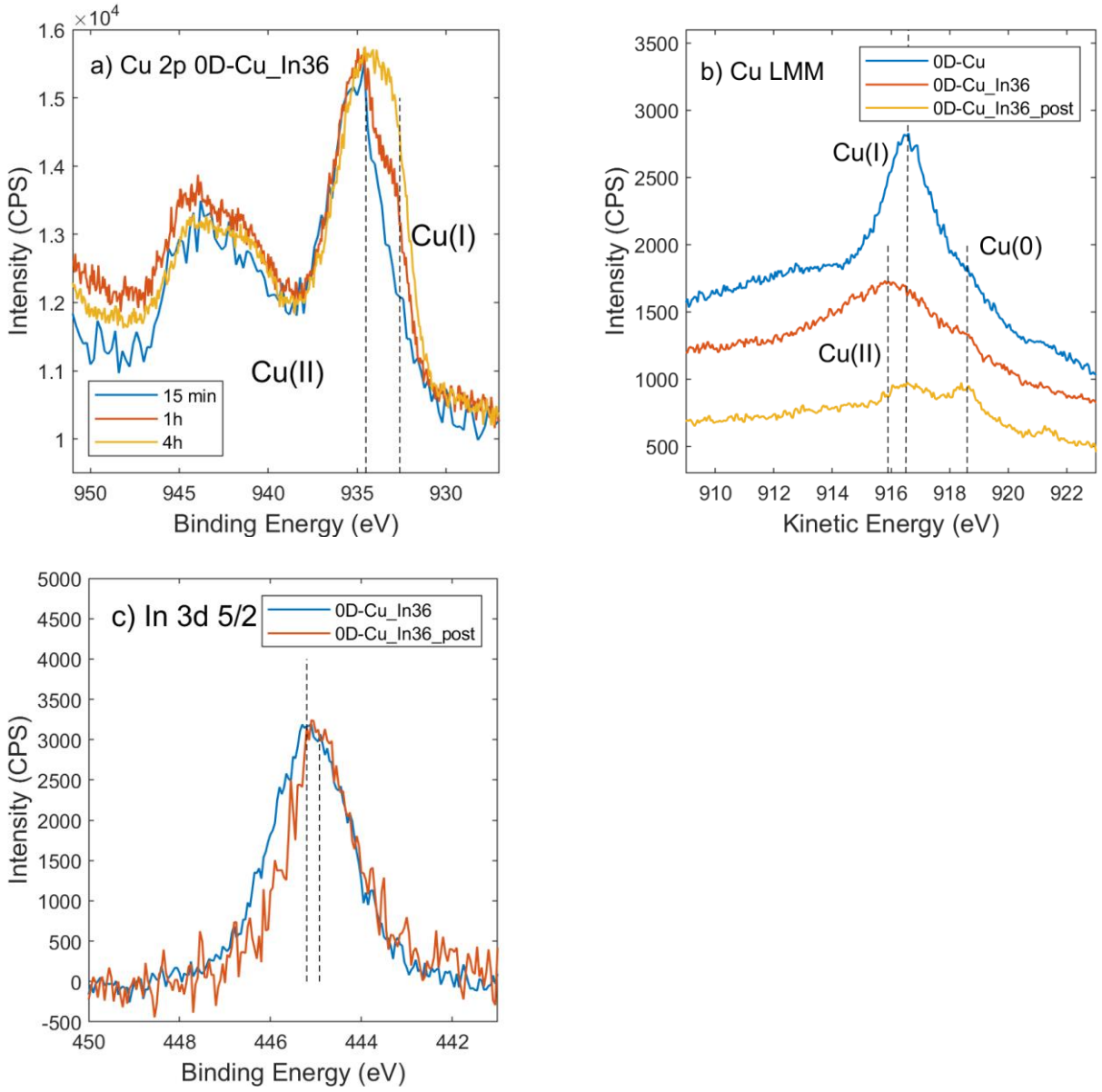

Figure S3. XPS signals of Cu 2p **(a)** as function of time, Cu LMM **(b)** and In 3d 5/2, where spectra were normalized and dotted lines at 445.2 eV and 444.9 eV were added **(c)**.

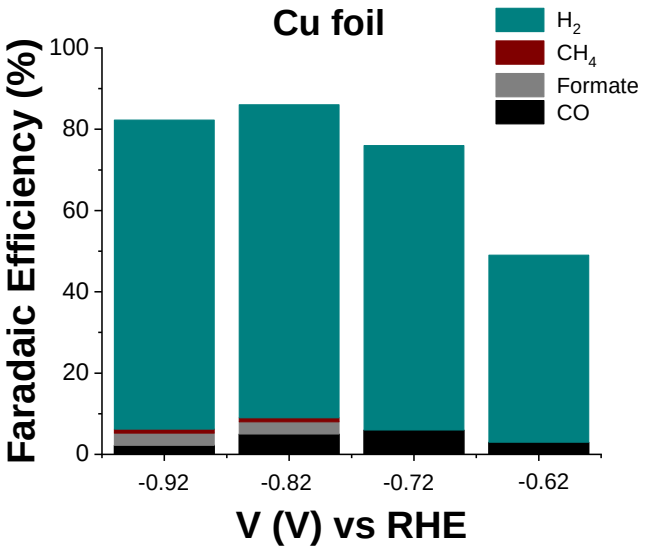
Cu foil
Faradaic Efficiency (%)
100
80
60
40
20
0
-0.92
-0.82
-0.72
-0.62
V (V) vs RHE
H2
CH4
Formate
CO

(a)

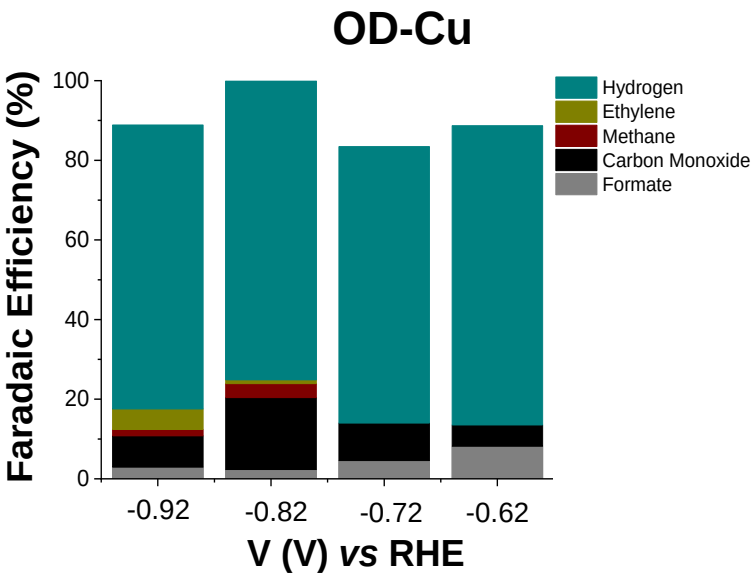
OD-Cu
Faradaic Efficiency (%)
100
80
60
40
20
0
-0.92
-0.82
-0.72
-0.62
V (V) vs RHE
Hydrogen
Ethylene
Methane
Carbon Monoxide
Formate

(b)

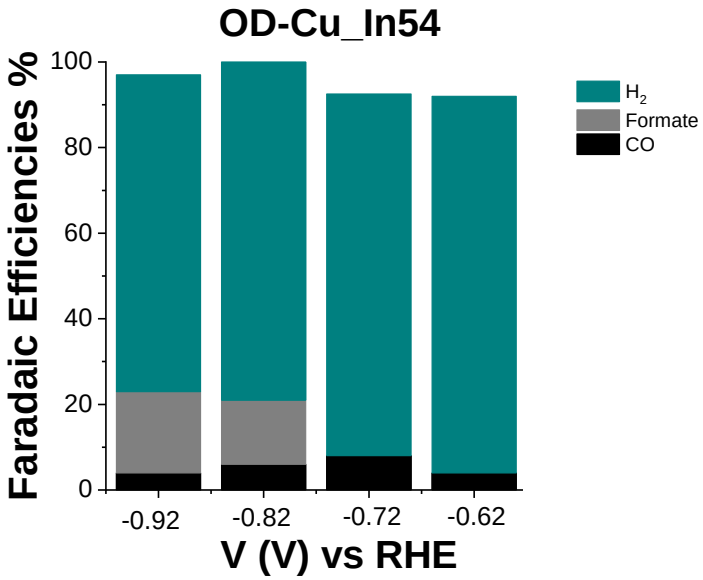
OD-Cu_In54
Faradaic Efficiencies %
100
80
60
40
20
0
-0.92
-0.82
-0.72
-0.62
V (V) vs RHE
H2
Formate
CO

(c)

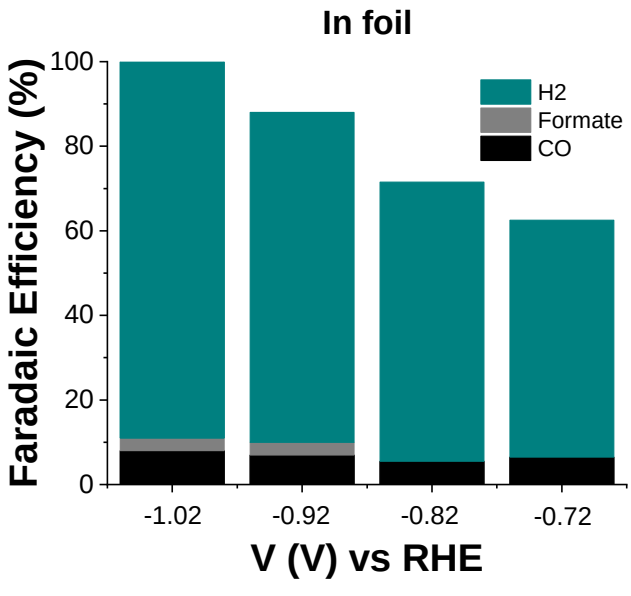

(d)

Figure S4. Faradic efficiency of the different products obtained with Cu foil **(a)**, OD-Cu **(b)**, OD-Cu_In54 **(c)** and In foil **(d)** cathodes as a function of the applied bias. Each bar is an average of at least two measurements. The <100% total FE observed at low potential (low current, i.e., lower amount of products) can be due to trapping of the gas products in stagnant corners of the electrochemical cell.

Table S3. Comparison of CO_2 reduction performance on different Cu-In catalysts.

Synthesis	**Morphology**	**Phase(s)**	**Products (% FE)** [a,b]	**J_{max}**	**Ref.**
Reductive electrodeposition of $In(NO_3)_3$ on OD-Cu (obtained by fast square wave anodization)	Textured nanocubes (<1 μm)	Cu/Cu_2O + $In(OH)_3$	@ -0.62 V vs RHE,[c]: * For OD-Cu_In36: syngas (46% H_2 and 48% CO => H_2/CO ratio ≈ 1) * For OD-Cu_In18: syngas (59% H_2 and 29% CO => H_2/CO ratio ≈ 2)	@ -0.62 V vs RHE: |J,tot| > 3.5 mA/cm^2	This work
Reductive electrodeposition of $InSO_4$ on OD-Cu (obtained by thermal oxidation)	Irregular grains (100-500 nm) from agglomeration of 50 nm nanoparticles	$Cu_{11}In_9$ alloy	@ -0.7 V vs RHE: CO (95%) HCOOH (ca. 3%) H_2 (<2%)	@ -0.7 V vs RHE: J,tot = -1.7 mA/cm^2	[1]

Near Infrared-driven decomposition of mixed metal precursors on Ti (different compositions obtained)	Nanoparticles (ca. 100 nm average diameter)	* For $Cu_{0.75}In_{0.25}$: Cu_2In phase	@ -0.7 V vs RHE,[d]: * For $Cu_{0.75}In_{0.25}$: CO (80%) H2 (20%)	@ -0.7 V vs RHE: J,CO ≈ -2 mA/cm^2	[2]
In situ reduction of: (a) $CuInO_2$ and (b) In_2O_3/Cu both deposited on carbon black	For both materials: Structural evolution during CO_2 reduction	Evolved catalyst (for both materials): Cu core + $In(OH)_3$ shell	For the evolved cat: @ -0.6 V vs RHE: CO (55%) $HCOO^-$ (ca. 5%) H_2 (ca. 40%)	@ -0.6 V vs RHE: J,CO ≈ -1 mA/cm^2 J,tot ≈ -1.8 mA/cm^2	[3]
Electrodeposition from $In_2(SO_4)_3$ + $CuSO_4$ on Au-sputtered Si. Different deposition potential results in different Cu/In ratios	Dendritic	* If In <25% → Cu(111) * If ca. 38% In → Cu_9In_4 and $Cu_{11}In_9$	@ -1 V vs RHE: * For 40% In: $HCOO^-$ (49%) syngas (36% H_2 and 14% CO => H_2/CO ratio = 2.6) * For 80% In: $HCOO^-$ (62%) CO (ca. 5%) H_2 (ca. 25%)	@ -0.8/-1.1 V vs RHE: J,$HCOO^-$ < -1 mA/cm^2	[4]
$Cu(OH)_2$ nanowires dipped in an $InCl_3$ solution + dehydration	Nanowires (10 μm av. length) with porous structure of Cu nanograins (10-30 nm) covered by a < 5 nm layer of In	Metallic Cu and metallic In	@-0.6 V vs RHE: * For 20% In: CO (93%) H_2 (ca. 4%) $HCOO^-$ (ca. 3%)	@ -0.6 V vs RHE: J,CO = -1.5 mA/cm^2	[5]
Electrochemical reduction of $CuInO_2$ deposited on carbon paper	Large particle aggregates with some small porosity	$Cu_{11}In_9$, Cu_7In_3 and Cu	@-0.8 V vs RHE: CO (70%) $HCOO^-$ (19%) H_2 (<10%)	@-0.8 V vs RHE: J,tot = -2 mA/cm^2	[6]

[a] Unless otherwise stated, all data are obtained in CO_2-saturated 0.1 M $KHCO_3$ aqueous solution; [b] Main product underlined; [c] Data obtained in CO_2-saturated 0.5 M $KHCO_3$ aqueous solution; [d] Data obtained in CO_2-saturated 0.5 M $NaHCO_3$ aqueous solution.

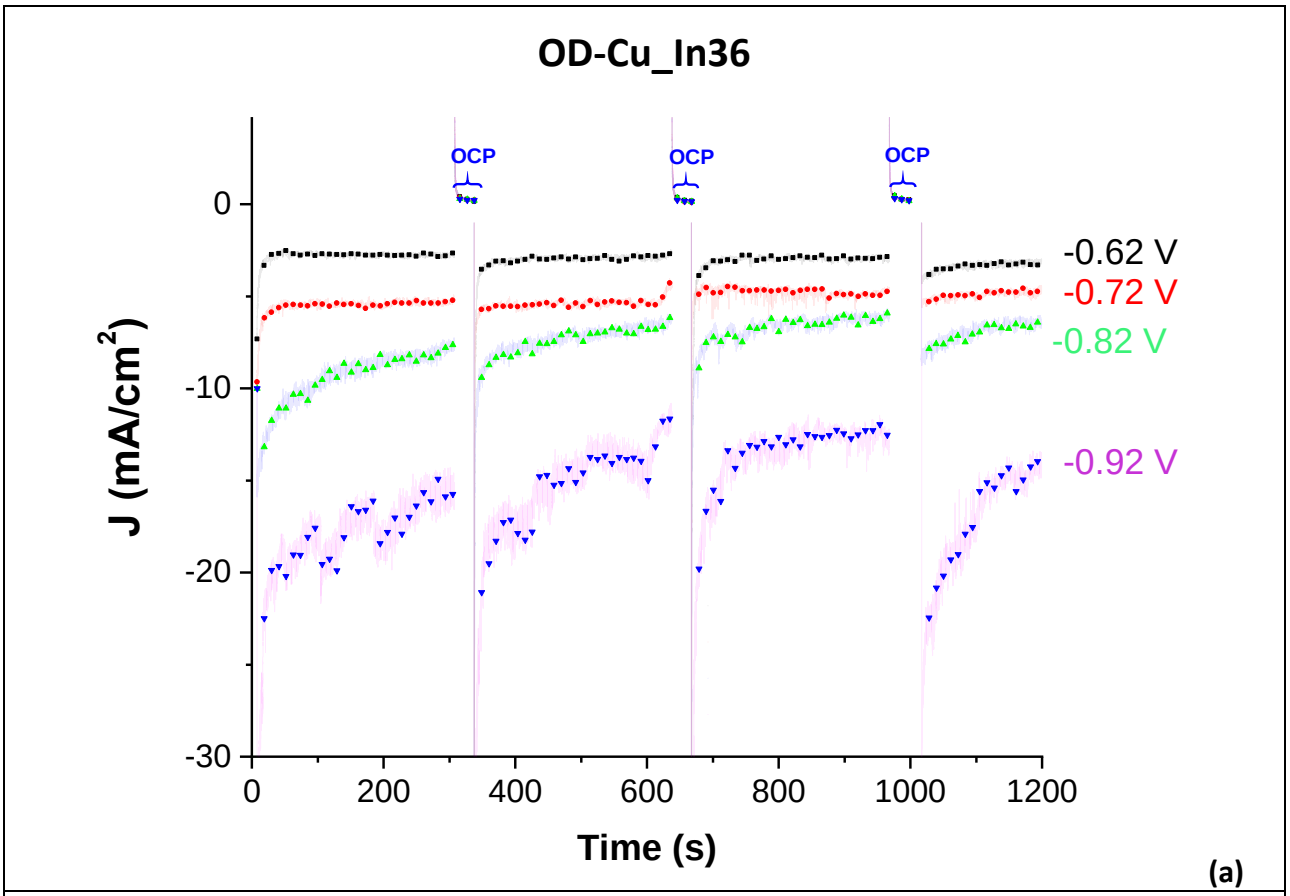
OD-Cu_In36
OCP
OCP
OCP
0
-10
-20
-30
J (mA/cm^2)
0
200
400
600
800
1000
1200
Time (s)
-0.62 V
-0.72 V
-0.82 V
-0.92 V
(a)

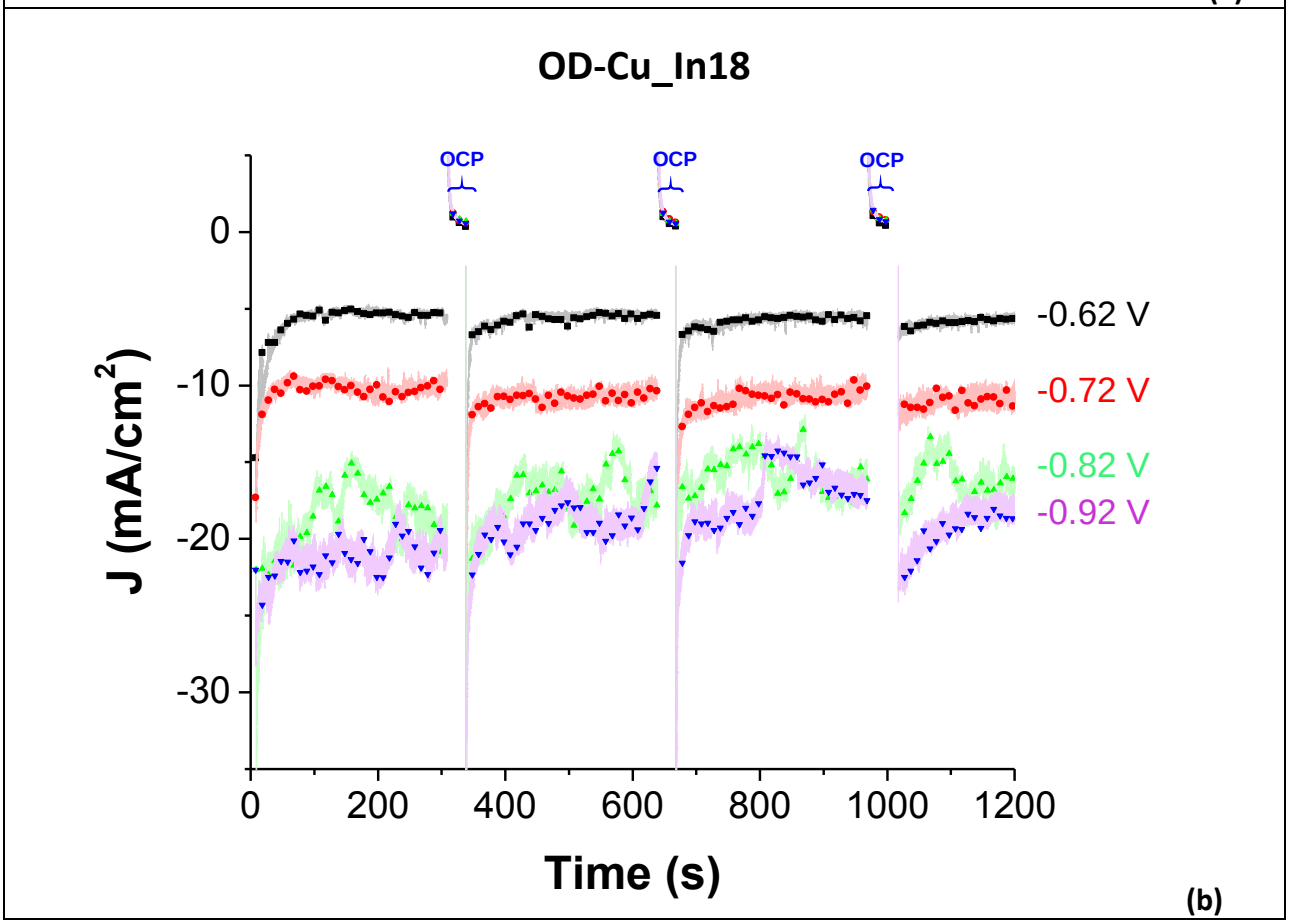
OD-Cu_In18
OCP
OCP
OCP
0
-10
-20
-30
J (mA/cm^2)
0
200
400
600
800
1000
1200
Time (s)
-0.62 V
-0.72 V
-0.82 V
-0.92 V
(b)

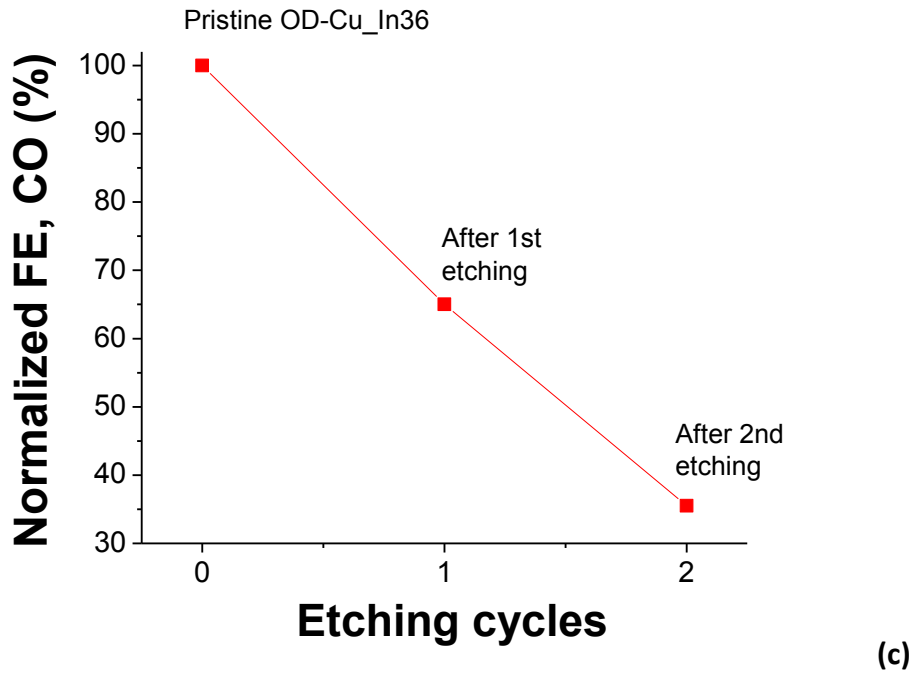

Figure S5. Stepped chronoamperometry experiments performed for the accumulation of the products obtained with OD-Cu_In36 **(a)** and OD-Cu_In18 **(b)**. In particular, the cathodes were stepped between the bias reported in the graphs (for 300 s) and the open circuit potential, OCP (for 40 s). **(c)** Faradaic efficiency for CO production for a pristine OD-Cu_In36 compared with those of the same cathode after 1 or 2 etching cycles aimed at removing the $In(OH)_3$ phase. Each etching cycle consists in 15-min immersion of the cathode in 1 M H_2SO_4 aqueous solution.

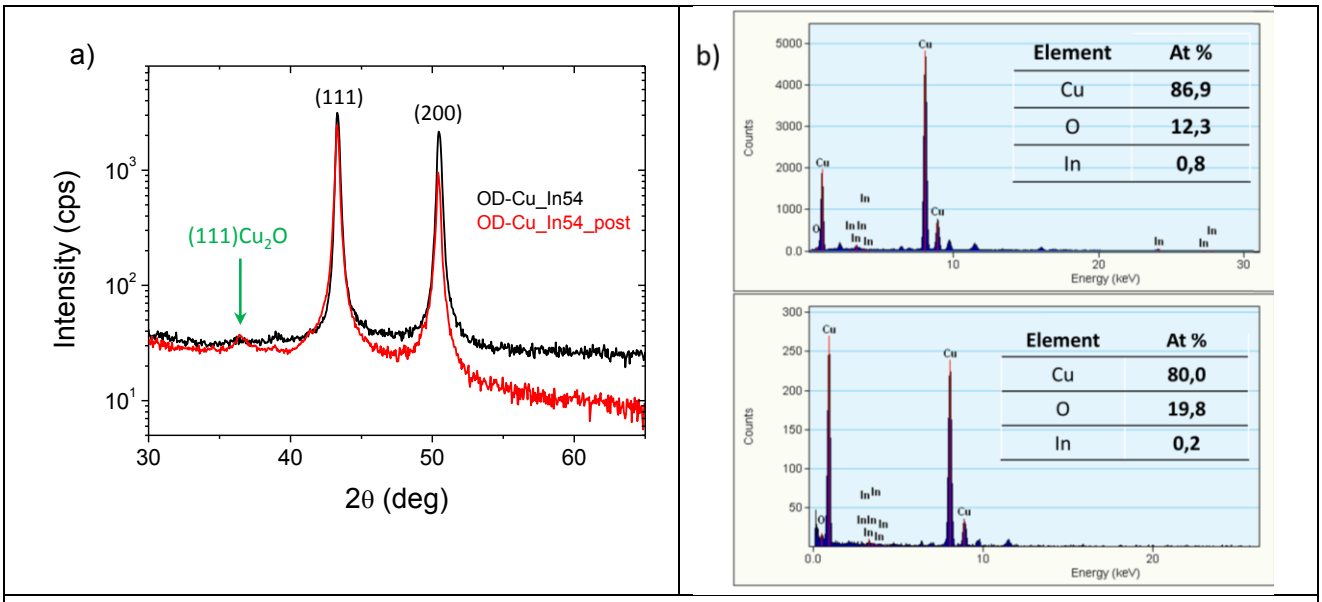

Figure S6. (a) Grazing-incidence X-ray diffractograms of OD-Cu_In54 before (black trace) and after (red trace) CO_2R experiments. **(b)** EDS spectra registered on a wide sample area identified by TEM, reporting relative Cu, O and In atomic content in the inset for OD-Cu_In54 before (top) and after (bottom) CO_2R experiments. Comparison based on OD-Cu_In54 sample to enhance the role of In-deposition on the materials structure upon exposure to CO_2R working conditions.

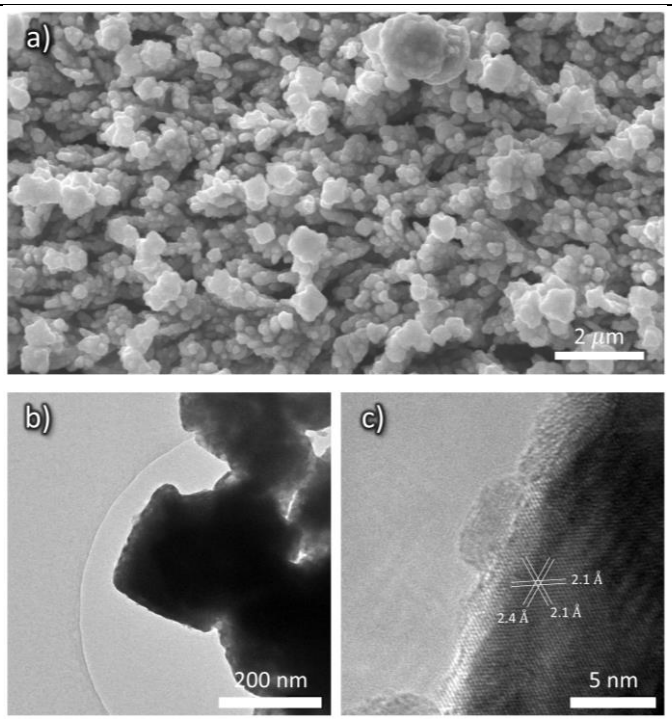

Figure S7. (a) SEM micrograph and **(b)** low or **(c)** high magnification HR-TEM micrographs of OD-Cu_In54 after CO_2R experiments. In the inset, d-spacing corresponding to lattice reflections compatible with Cuprite phase.

References:

[1] S. Rasul, D. H. Anjum, A. Jedidi, Y. Minenkov, L. Cavallo and K. Takanabe, *Angewandte Chemie*, 2015, **127**, 2174-2178

[2] J. He, K. E. Dettelbach, D. A. Salvatore, T. Li and C. P. Berlinguette, *Angewandte Chemie*, 2017, **129**, 6164-6168

[3] G. n. O. Larrazábal, A. J. Martín, S. Mitchell, R. Hauert and J. Pérez-Ramírez, *ACS Catalysis*, 2016, **6**, 6265-6274

[4] Z. B. Hoffman, T. S. Gray, K. B. Moraveck, T. B. Gunnoe and G. Zangari, *ACS Catalysis*, 2017, **7**, 5381-5390

[5] W. Luo, W. Xie, R. Mutschler, E. Oveisi, G. L. De Gregorio, R. Buonsanti and A. Züttel, *ACS Catalysis*, 2018, **8**, 6571-6581

[6] A. Jedidi, S. Rasul, D. Masih, L. Cavallo and K. Takanabe, *Journal of Materials Chemistry A*, 2015, **3**, 19085-19092